

A SLOW MERGER HISTORY OF FIELD GALAXIES SINCE $Z \sim 1$ ¹KEVIN BUNDY², MASATAKA FUKUGITA³, RICHARD S. ELLIS², TADAYUKI KODAMA⁴,
CHRISTOPHER J. CONSELICE²

kbundy@astro.caltech.edu, fukugita@sdss1.icrr.u-tokyo.ac.jp, rse@atro.caltech.edu, kodama@th.nao.ac.jp, cc@astro.caltech.edu

To Be Published in ApJ Letters

ABSTRACT

Using deep infrared observations conducted with the CISCO imager on the Subaru Telescope, we investigate the field-corrected pair fraction and the implied merger rate of galaxies in redshift survey fields with Hubble Space Telescope imaging. In the redshift interval, $0.5 < z < 1.5$, the fraction of infrared-selected pairs increases only modestly with redshift to $7\% \pm 6\%$ at $z \sim 1$. This is nearly a factor of three less than the fraction, $22\% \pm 8\%$, determined using the same technique on *HST* optical images and as measured in a previous similar study. Tests support the hypothesis that optical pair fractions at $z \sim 1$ are inflated by bright star-forming regions that are unlikely to be representative of the underlying mass distribution. By determining stellar masses for the companions, we estimate the mass accretion rate associated with merging galaxies. At $z \sim 1$, we estimate this to be $2 \times 10^{9 \pm 0.2} M_{\odot} \text{ galaxy}^{-1} \text{ Gyr}^{-1}$. Although uncertainties remain, our results suggest that the growth of galaxies via the accretion of pre-existing fragments remains as significant a phenomenon in the redshift range studied as that estimated from ongoing star formation in independent surveys.

Subject headings: galaxies: evolution — galaxies: interactions — galaxies: stellar content

1. INTRODUCTION

The hierarchical growth of dark matter halos is thought to govern the assembly history and morphological evolution of galaxies. Nearby examples of interacting and merging galaxies are well known, and many attempts to survey the merging and mass accretion rate at various redshifts have been made by several groups (Burkey, Keel, & Windhorst 1994; Carlberg, Pritchett, & Infante 1994; Yee & Ellingson 1995; Patton et al. 1997; Le Fèvre et al. 2000; Patton et al. 2000, 2002; Conselice et al. 2003). Strong evolution of the global merger rate was used to explain the observed faint galaxy excess (Broadhurst, Ellis, & Glazebrook 1992), the evolution of the luminosity function (Lilly et al. 1995; Ellis et al. 1996), and that of galaxy morphologies (Giavalisco et al. 1996; Brinchmann et al. 1998). Evolution of the merger rate can also be used to place constraints on structure formation (Baugh, Cole, & Frenk 1996; Kauffmann 1996).

Le Fèvre et al. (2000) used Hubble Space Telescope (*HST*) F814W images of redshift survey fields to measure the pair fraction to $z \sim 1$. They found an increase in the field-corrected pair fraction to 20% at $z \sim 0.75$ -1. However, as Le Fèvre et al. discuss, various biases affect this result. For example, in the rest-frame blue, bright star-forming regions, possibly triggered by interactions, might inflate the significance of pair statistics and give a false indication of the mass assembly rate.

Infrared observations are less biased by star formation, and serve as a better tracer of the underlying stellar mass in galaxies (Broadhurst, Ellis, & Glazebrook 1992). Dickinson et al. (2003) employed this in their investigation of the global stellar mass density for $z < 3$. They find that

50 to 70% of the present-day stellar mass was in place by $z \sim 1$. A second line of evidence, the decline from $z \sim 1$ to 0 in the global star formation rate (e.g., Lilly et al. 1996), provides further support for the contention that galaxy growth was not yet complete at $z \sim 1$. Though a chronological picture of stellar mass assembly is emerging, the processes driving it are not understood. Is star-formation and stellar mass assembly induced mainly through the gradual accretion of gas converted quiescently into stars, or does assembly occur through merging, potentially accompanied by tidally-induced star formation? Characterizing the continued growth of galaxies, and specifically the contribution from galaxy mergers since $z \sim 1$, is the major goal of this work.

2. OBSERVATIONS

In addition to high resolution infrared imaging, this study relies on optical *HST* data to facilitate the comparison between infrared and optical pair statistics and constrain stellar M/L_K ratios used to infer the stellar mass accretion rate. We therefore selected fields for our K' -band imaging campaign that contain a combination of statistically-complete redshift surveys and archival *HST* F814W imaging. Target galaxies of known redshift were selected from the RA=10hr field of the CFRS (Lilly et al. 1995), which spans the apparent magnitude range $17.5 < I_{AB} < 22.5$, and the Groth Strip area, surveyed by the Deep Extragalactic Evolutionary Probe (DEEP; Koo 1995) and selected according to $(R+I)/2 < 23$ (Koo 2000, private communication).

Archival *HST* images of the Groth Strip, retrieved from two programs (GTO 5090, PI: Groth; GTO 5109, PI: Westphal), reach $I \approx 24$ (Groth et al. 1994), a depth suf-

¹ Based on data acquired at the Subaru Telescope, which is operated by the National Astronomical Observatory of Japan.

² 105–24 Caltech, 1201 E. California Blvd., Pasadena, CA 91125

³ Institute for Cosmic Ray Research, University of Tokyo, Kashiwa 277 8582, Japan

⁴ National Astronomical Observatory of Japan, Mitaka, Tokyo 181–8588, Japan

ficient for us. The deeper *HST* images of the CFRS fields ($I < 24.5$) are described by Brinchmann et al. (1998).

K' -band observations were performed using the CISCO imager (Motohara et al. 2002) on the Subaru telescope during two campaigns in 2002 April and 2003 April. The camera has a field of 108 arcsec on a side with the pixel size of 0.11 arcsec, and is thus fairly well-matched to that of WFPC2. Field centers were chosen to maximize the number of galaxies of known redshift falling within the CISCO field of view. Given we are concerned with counting satellites around individual hosts, our primary results will not be biased by this maximization.

In total, six Groth Strip and four CFRS fields were imaged to a depth (~ 2.6 ks) deemed adequate for locating galaxies at least 2 magnitudes fainter than most of the hosts (see below). In total, 190 redshift survey galaxies were sampled in the K' -band (151 fully overlap with *HST* images and are bright enough for the comparison to the optical pair fraction). The infrared data were reduced using the AUTOMKIM pipeline developed at the Subaru facility by the CISCO group.

The limiting depth for locating faint satellites was estimated by performing photometry on artificial stars inserted into each image and by comparing the observed galaxy number counts to those published by Djorgovski et al. (1995). Both techniques agree, demonstrating that the CISCO data are complete at the 90% level at $K = 22.5$. Object detection and photometry in both the optical and infrared were carried out using the SExtractor package (Bertin & Arnouts 1996).

3. OPTICAL VERSUS INFRARED-SELECTED PAIR FRACTIONS

First, we compare the optical and infrared pair fractions, closely following the precepts of Le Fèvre et al. (2000), though we adopt the cosmology— $\Omega_M = 0.3$, $\Lambda = 0.7$, and $h = 0.7$ —instead of $q_0 = 0.5$ and $h = 0.5$ as used by Le Fèvre et al. Pairs are identified as companions to a limit no more than 1.5 magnitudes (independently in both optical and K' -band) fainter than their host galaxy within a separation radius of $r_p = 20$ kpc. Satellites within this radius are expected to strongly interact with the halo of the host and merge in less than ~ 1 Gyr due to dynamical friction (Patton et al. 1997). Multiple satellites around the same host are counted as separate pairs, and a field correction is applied to the pair counts based on the observed number density. Throughout, we assume that the pair fraction is independent of the intrinsic properties of the host galaxies and the way they were selected.

The field-corrected optical and infrared pair fractions for a sample of 151 host galaxies of known redshift with $K < 21$ and $I < 23$ are presented in Figure 1 and Table 1 and contrasted with the results using the same optical procedure as derived from Table 3 of Le Fèvre et al. (2000). Our first redshift bin ($0.2 < z < 0.5$) contains too few hosts for useful comparisons, but in the two higher redshift bins ($0.5 < z < 0.75$ and $0.75 < z < 1.5$), the statistical significance is adequate. There, although we find optical results comparable to Le Fèvre et al. (2000), the infrared pair fraction is a factor of 2-3 less. See Figure 2 for some examples.

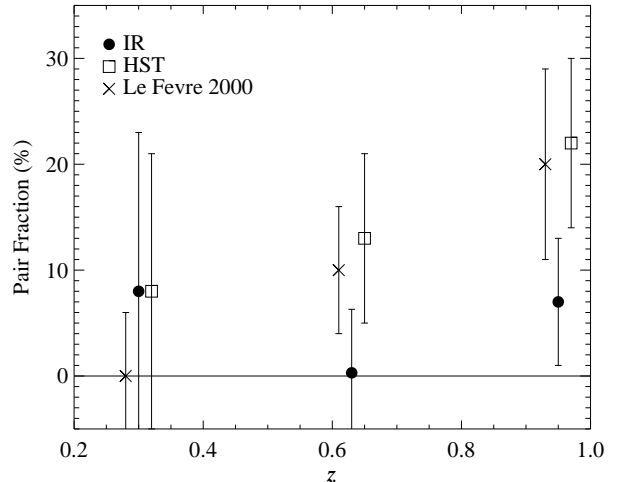


FIG. 1.— The field-subtracted pair fraction as measured in the infrared and optical. K' -band measurements appear as filled circles and *HST* F814W measures as squares. The new results are compared with those of Le Fèvre et al. (2000).

To examine the possibility that our comparison with an equivalent *HST* analysis may be biased by resolution effects, we convolve each $0''.1$ *HST* image to the corresponding CISCO resolution, which varies from $0''.35$ to $0''.5$. We then repeat the detection and analysis, including the background number counts. The *HST* pair fraction decreases by only $\sim 30\%$, remaining a factor of two above the infrared pair fractions in the two highest redshift bins. We also investigate the separation distribution between each optical companion and its host. The smallest separation is just above $0''.5$, implying that the majority of optically-identified pairs would be readily resolved in the CISCO images, but were simply too faint in the infrared to be counted. Both results suggest that resolution is not the primary difference between the two samples, rather it is the bluer colors of the satellite galaxies. In general, observed satellite galaxies tend to be bluer in $(V - K)$ than hosts, though the detection in IR favors redder companions.

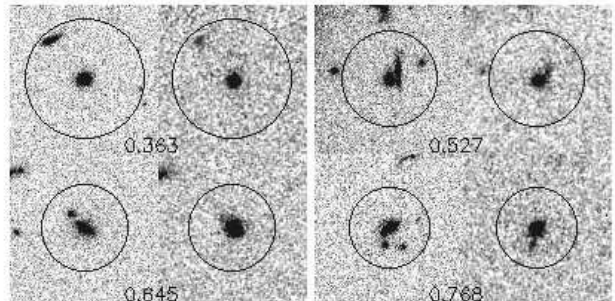


FIG. 2.— Examples of pairs identified in the optical but not in the infrared. In each set, the left postage stamp is from *HST* I_{814} , and the right is from CISCO K' -band images. The 20 kpc radius and redshifts are indicated.

4. WEIGHTED INFRARED PAIR STATISTICS

We now explore a more detailed formalism for investigating the merger history as laid out by Patton et al. (2000). Rather than applying a differential magnitude cut linked to the host galaxy, we select companions in a fixed

absolute magnitude range, $-24 \leq M_{K'} \leq -19$, regardless of the host. This will increase the number of observed pairs since we include fainter companion galaxies. Our sample for this analysis also grows to 190 hosts because host galaxies with $21.0 < K' < 22.5$ are now included.

As in §3, the companion search radius is set to $r_p = 20$ kpc and field subtraction implemented as before. Absolute magnitudes are calculated using k -corrections for the K' -band tabulated by Poggianti (1997) (using the Sa model), assuming that each companion galaxy is at the same redshift as its host.

A volume-limited estimate of the pair fraction as a function of redshift can be achieved by applying weights to both companions and hosts. As it is easier to detect intrinsically fainter galaxies nearby, higher redshift companions must be given more weight. The opposite is true for host galaxies because the observed number of pairs per host is less certain at higher redshift. Following Patton et al. (2000), these weights are based on the comoving density of companions observed in a hypothetical volume-limited survey compared to that in a flux-limited survey. We calculate these weights by integrating K' (or K_s) band luminosity functions from Cole et al. (2001), for $z < 0.6$, and Kashikawa et al. (2003), for $0.6 < z < 1.5$.

The results are given in Table 2. At $z \sim 1$, the merger fraction of $24\% \pm 10\%$ is expectedly higher because of the inclusion of fainter galaxies. The errors are derived from counting statistics, and as in §3, we expect the true pair fraction to be slightly higher (about 1%) than observed because some faint companions may be obscured by large hosts. The implied merger rate suggests that 35% of typical L^* galaxies have undergone a merger with a companion in this luminosity range since $z \sim 1$.

5. MASS ASSEMBLY RATES

We have applied two pair counting methods and found that the Patton et al. method delivers a pair fraction higher than the technique of Le Fèvre et al. because the former includes fainter companions. To reconcile these two different results with a single mass assembly history, we estimate the stellar mass accretion rate associated with merging galaxies. Because it is not known which companions are physically associated with their host, the stellar mass of companions can only be determined in a statistical sense. We first fit our VIK' photometry of host galaxies (with redshifts) to template SEDs spanning a range of ages, star formation histories, and metallicities, assuming a Salpeter IMF (with the range $0.1 - 100 M_\odot$, Bruzual & Charlot 2000, private communication). We then scale to the K' -band luminosity to estimate the stellar mass (see Brinchmann et al. 2000). We assume the companions follow the same distribution of $M_*/L_{K'}$ vs. $L_{K'}$ as the hosts and use this distribution to estimate the stellar mass of companion galaxies. Finally, though the merging timescale depends on the details of the interaction, we follow previous studies (e.g., Patton et al. 2000) and assume an average value of 0.5 Gyr for galaxies separated by $r_p < 20$ kpc.

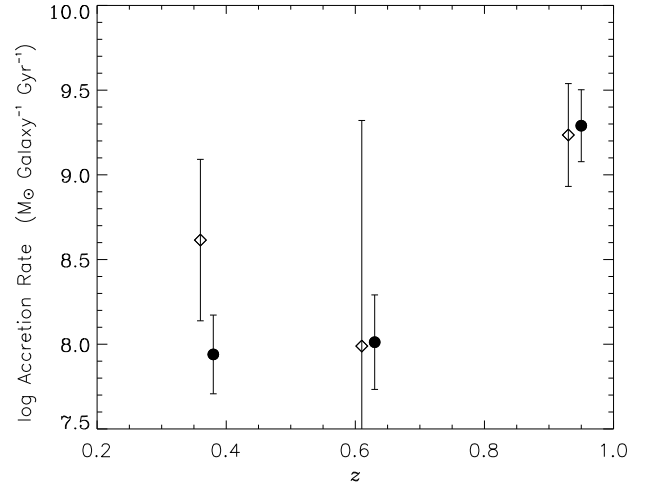


FIG. 3.— Stellar mass accretion rate per galaxy in three redshift bins. Filled symbols are the results from the Patton et al. weighted analysis. Open symbols are the results of the Le Fèvre et al. technique. The first redshift bin is again the least significant since it contains the fewest host galaxies.

With these assumptions, we demonstrate that the two very different pair statistics are consistent with a similar merger history in terms of the accreted stellar mass. In Figure 3, open symbols are the mass accretion rate from the Le Fèvre et al. method, and solid symbols are that from the Patton et al. method. The large error bars include both statistics and 50% uncertainties in $M_*/L_{K'}$. Both methods illustrate a rise in the stellar mass accretion rate at the highest redshifts, with the Patton et al. method giving a value of $2 \times 10^{9 \pm 0.2} M_\odot \text{ galaxy}^{-1} \text{ Gyr}^{-1}$ at $z \sim 1$. This mass corresponds to $\approx 4\%$ of the average stellar mass of host galaxies at these redshifts. The result may be compared with an estimate made by Conselice et al. (2003) of $6.4 \times 10^{8 \pm 0.1} M_\odot \text{ galaxy}^{-1} \text{ Gyr}^{-1}$ at $0.8 < z < 1.4$ using morphological indicators to distinguish merger remnants.

We contrast our assembly rate from pre-existing stellar systems with the *integrated* stellar mass density (Dickinson et al. 2003), which reflects the growth of galaxies from newly-formed stars. While not necessarily completely independent (for example if merging triggers new star formation), the relative magnitudes of the two phenomena are interesting to consider. Using the luminosity functions of Kashikawa et al (2003) to determine the comoving number density of host galaxies, we integrate the mass accretion rate to estimate the stellar mass assimilated by galaxies in the host K-band luminosity range, finding $\Delta \rho_*^m \approx 3 \times 10^{8 \pm 0.2} M_\odot \text{ Mpc}^{-3}$. For a Salpeter IMF, we deduce that 30% of the local stellar mass in luminous galaxies was assimilated via merging of pre-existing stars since $z \sim 1$, comparable to the build-up deduced by Dickinson et al. (2003) from ongoing star formation.

We thank Chris Simpson and Kentaro Aoki for their help during our observations at the Subaru Telescope. RSE and MF acknowledge the generosity of the Japanese Society for the Promotion of Science.

REFERENCES

- Baugh, G., Cole, S. & Frenk, C. S. 1996, MNRAS, 283, 1361
 Bertin, E. & Arnouts, S. 1996, A&A, 117, 393
 Brinchmann, J. & Ellis, R. S. 2000, ApJ, 546, L77
 Brinchmann, J., et al. 1998, ApJ, 499, 112
 Broadhurst, T. J., Ellis, R. S., & Glazebrook, K. 1992, Nature, 355, 55
 Burkey, J. M., Keel, W. C., & Windhorst, R. A. 1994, ApJ, 429, 13
 Carlberg, R. G., Pritchet, C. J., & Infante, L. 1994, ApJ, 435, 540
 Cole, S., et al. 2001, MNRAS, 326, 255
 Conselice, C. J., Bershady, M. A., Dickinson, M., & Papovich, C. 2003, ApJ, 126, 1183
 Dickinson, M., Papovich, C., Ferguson, H. C., & Budávári, T. 2003, ApJ, 587, 25
 Djorgovski, S. et al. 1995, ApJ, 438, L13
 Ellis, R. S., Colless, M., Broadhurst, T., Heyl, J., & Glazebrook, K. 1996, MNRAS, 280, 235
 Giavalisco, M., Livio, M., Bohlin, R. C., Macchetto, F. D., & Stecher, T. P. 1996, AJ, 112, 369
 Groth, E. J., Kristian, J. A., Lynds, R., O’Neil, E. J., Balsano, R., & Rhodes, J. 1994, BAAS, 26, 1403
 Kashikawa, N., et al. 2003, AJ, 125, 53
 Kauffmann, G. 1996, MNRAS, 281, 475
 Koo, D. C. 1995, in Wide Field Spectroscopy and the Distant Universe, ed. S. Maddox & Aragón-Salamanca (Singapore: World Scientific), 55,
 Le Fèvre, O., et al. 2000, MNRAS, 311, 565
 Lilly, S. J., Le Fèvre, O., Crampton, D., Hammer, & F., Tresse, L. 1995, ApJ, 455, 50
 Lilly, S. J., Le Fèvre, O., Hammer, & F., & Crampton, D., 1996, ApJ, 460, L1
 Motohara, K., et al. 2002, PASJ, 54, 315
 Patton, D. R., Carlberg, R. G., Marzke, R. O., Pritchet, C. J., da Costa, L. N., & Pellegrini, P. S. 2000, ApJ, 536, 153
 Patton, D. R., et al. 2002, ApJ, 565, 208
 Patton, D. R., Pritchet, C. L., Yee, H. K. C., Ellingson, E., & Carlberg, R. G. 1997, ApJ, 475, 29
 Poggianti, B. M. 1997, A&A, 122, 399
 Yee, H. K. C., & Ellingson, E. 1995, ApJ, 445, 37

TABLE 1
PAIR FRACTION

Sample	z	N_{gal}	N_{maj}	N_{proj}	Pair Fraction (%)	Merger Fraction (%)
CISCO	0.2–0.5	22	6 (0.27)	4.4 (0.20)	8 ± 14	4 ± 10
CISCO	0.5–0.75	47	4 (0.09)	3.8 (0.08)	0.3 ± 6	0.2 ± 5
CISCO	0.75–1.5	74	11 (0.15)	5.8 (0.08)	7 ± 6	7 ± 6
HST F814W	0.2–0.5	22	5 (0.23)	3.3 (0.15)	8 ± 13	5 ± 8
HST F814W	0.5–0.75	47	10 (0.21)	4.0 (0.09)	13 ± 8	11 ± 7
HST F814W	0.75–1.5	74	25 (0.34)	8.5 (0.11)	22 ± 8	21 ± 8
Le Fèvre	0.2–0.5	98	11 (0.11)	19 (0.19)	0	0
Le Fèvre	0.5–0.75	89	21 (0.24)	12.2 (0.14)	9.9 ± 6	8 ± 5
Le Fèvre	0.75–1.3	62	21 (0.34)	8.4 (0.14)	20.3 ± 9	19.4 ± 9

Note. — N_{gal} is the total number of galaxies drawn from the redshift sample. N_{maj} is the number of companions fitting the pair criteria described in the text. N_{proj} is the expected number of contaminating field galaxies. The pair fraction is defined as $(N_{maj} - N_{proj})/N_{gal}$ and the merger fraction is the pair fraction corrected by a factor of $0.5(1+z)$ where $(1+z)$ corresponds to the mean redshift of the bin. Numbers appearing in parentheses are the averages per host galaxy, printed for comparison to N_c^D and N_c^R in Table 2. Results from ‘All CFRS+LDSS’ in Table 3 of Le Fèvre et al. (2000) are also reproduced. Errors are calculated using counting statistics.

TABLE 2
WEIGHTED PAIR STATISTICS

z	N_{gal}	N_c^D	N_c^R	N_c	Average M_K	Merger Fraction
0.2–0.5	30	0.18	0.04	0.14 ± 0.07	-17.9	12 ± 5
0.5–0.75	57	0.11	0.04	0.08 ± 0.06	-18.3	8 ± 5
0.75–1.5	93	0.29	0.03	0.26 ± 0.10	-20.5	24 ± 10

Note. — N_{gal} is the total number of galaxies drawn from the redshift sample. N_c^D is the raw, weighted number of companions per host while N_c^R is the projected fraction from the field. The corrected average is N_c . The average M_K is the associated K' -band luminosity in companions averaged over every host in the sample. The merger fraction is calculated as before. Errors are determined using weighted counting statistics.